Energy scalable terahertz-wave parametric oscillator using surface-emitted configuration

Tomofumi Ikari
ikari@riken.jp
RIKEN Advanced Science Institute, 519-1399, Aramaki Aoba, Aoba-ku, Sendai 980-0845, Japan

Ruixiang Guo
RIKEN Advanced Science Institute, 519-1399, Aramaki Aoba, Aoba-ku, Sendai 980-0845, Japan

Hiroaki Minamide
RIKEN Advanced Science Institute, 519-1399, Aramaki Aoba, Aoba-ku, Sendai 980-0845, Japan

Hiromasa Ito
RIKEN Advanced Science Institute, 519-1399, Aramaki Aoba, Aoba-ku, Sendai 980-0845, Japan
Graduate School of Engineering, Tohoku University, Sendai 980-8577, Japan

We experimentally demonstrated the scalability of the terahertz (THz)-wave parametric oscillator by using a pump beam with a wide aperture and a high pulse energy. THz-wave absorption by the $LiNbO_3$ crystal in the oscillator is substantially suppressed by employing a surface-emitting cavity configuration. We also improved the conversion efficiency by increasing the parametric interaction in the noncollinear phase-matching geometry. A pump depletion of 54% and a conversion efficiency of 0.9×10^{-6} are achieved. A maximum THz output of 382 nJ/pulse was achieved at 1.46 THz using a 8.0 mm-diameter pump beam with a pulse energy of 465 mJ/pulse. [DOI: 10.2971/jeos.2010.10054]

Keywords: terahertz-wave, parametric oscillation, surface emission, energy enhancement

1 INTRODUCTION

Over the last two decades, many THz applications have been proposed in an increasingly wide variety of fields, including information and communication technology, biology and medical science, nondestructive evaluation and national security [1]–[5]. High-power widely tunable THz sources are required in practical applications of THz technologies. For instance, security imaging at airports requires high power to achieve enough penetration through clothing and luggage to be able to identify weapons and possibly explosives in real-time.

We have focused on developing widely tunable THz parametric sources that use phonon-polariton scattering in a $LiNbO_3$ crystal [6]–[8]. These sources can generate monochromatic radiation in the frequency range 1 THz–3 THz at room temperature. Several schemes have been implemented to enhance the THz-wave output energy. Output energy enhancement using a Si prism array and an injection technique has been demonstrated [9]. A Si prism coupler not only increases the output energy but it also generates unidirectional radiation with frequencies in the range 1 THz–3 THz, enabling THz-wave parametric oscillators (TPOs) to be used for spectroscopic and multifrequency imaging [3, 10]. The output energy and parametric gain have been increased by cryogenically cooling $LiNbO_3$ [11]. An enhanced efficiency was achieved by using $LiNbO_3$ waveguide confinement [12]. A top-hat pump beam was shown to enhance the THz-wave from a THz–wave parametric generator [13].

Using high-energy pumping in conjunction with a large pump spot size is effective for enhancing the output energy in non-collinear phase matching geometry [14]. However, in conventional THz-wave parametric generators, the high absorption loss in the $LiNbO_3$ crystal prevents energy up-scaling. Furthermore, up-scaling TPOs has not been investigated.

In this report, we investigate increasing the output energy and the efficiency of a surface-emitting (SE) TPO by simultaneously increasing the aperture size for the pump beam and using a higher pump beam energy. In the SE configuration, a THz wave is emitted from the surface at which the pump and idler beams reflect [15]. Thus, the area from which THz radiation is emitted from can be scaled by varying the pump spot size. Both the conversion efficiency and the output energy were increased by this technique. By performing experiments using several spot sizes of the pump beam, we demonstrate that these enhancements in the output energy and efficiency are due to increasing the interaction volume in a non-collinear geometry.

2 EXPERIMENTAL SETUP

Figure 1(a) shows the experimental set-up for our SE-TPO which is configured from two rectangular and one trapezoidal MgO:$LiNbO_3$ crystals. The two rectangular crystals were placed on either side of the trapezoidal crystal. The *c*-axes of these crystals are parallel to each other. The end surfaces that the pump and idler beams pass through were antireflection coated for the wavelengths of the pump and idler beams, respectively. The pump laser was a Q-switched Nd:YAG laser with an output wavelength of 1.064 μm. The

Received April 16, 2010; published November 08, 2010

ISSN 1990-2573

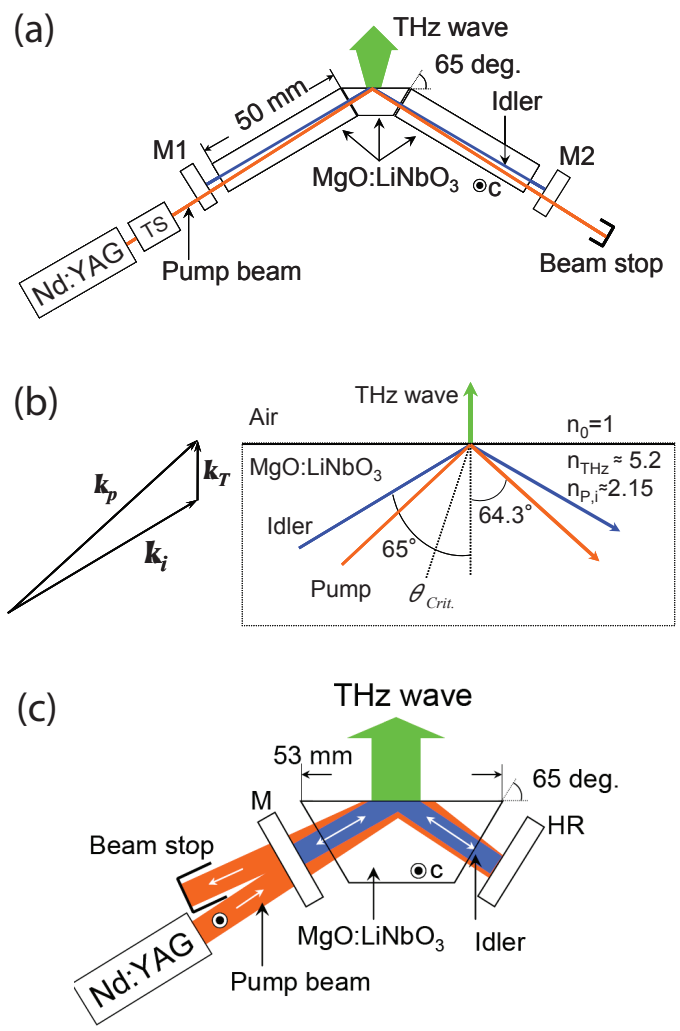

FIG. 1 (a) Schematic diagram of SE-TPO. M_1 and M_2: cavity mirrors, TS: telescope. (b) The noncollinear phase matching condition (left) and schematic diagram of three beams for the perpendicular generation at 1.5 THz (right). $\mathbf{k}_p$, $\mathbf{k}_i$, and $\mathbf{k}_T$ show the wave vectors of the pump, idler and THz, respectively. (c) Schematic diagram of SE-TPO enabling a larger pump beam and high energy pumping. The cavity is based on the off-axis pump double-pass singly resonant oscillator.

polarization of the pump beam was parallel to the *c*-axes of the crystals. Two flat cavity mirrors, M_1 and M_2, were used for the idler wave resonance. These cavity mirrors were specially fabricated to have a high transmittance at 1.064 μm and a high reflectivity above 1.068 μm. To enable higher energy pumping, an amplified longitudinal multimode Nd:YAG laser was used that can generate pulses with energies of up to 80 mJ/pulse and with a pulse length of 25 ns. The pump beam was compressed or expanded using a Galilean-telescope configuration to produce collimated beams with full width half maximum (FWHM) diameters of 1.0 mm, 1.7 mm and 2.2 mm.

THz waves were generated normal to the output surface by setting the incident angles of the pump and idler beams to the crystal surface as shown in Figure 1(b). In the polariton-scattering process, idler (Stokes) and signal (THz) waves are generated from the pump (near-infrared) wave in a direction consistent with noncollinear phase-matching, $\mathbf{k}_p = \mathbf{k}_i + \mathbf{k}_T$, where $\mathbf{k}_p$, $\mathbf{k}_i$, and $\mathbf{k}_T$ are the wave vectors of the pump, idler, and THz waves, respectively. Figure 1(b) shows incident angles of pump and idler beams to the crystal surface. For perpendicular emission at 1.5 THz, the idler beam incident angle is set to 65°, (i.e. the phase-matching angle, $\delta_{1.5\mathrm{THz}}$) for 1.5 THz generation and the pump beam incident angle is set to 64.3° (i.e. $\delta_{1.5\mathrm{THz}} - \theta_{1.5\mathrm{THz}}$). These angles exceed the critical angle ($\theta_{\mathrm{crit}} = 27.7°$) of the interface between the $MgO:LiNbO_3$ crystal ($n_{p,I} \approx 2.15$) and air ($n = 1$), ensuring that both the idler and pump beams are totally reflected at the surface.

We designed another SE-TPO cavity that had a much higher pumping energy and a wider pump beam size, as shown in Figure 1(c). An isosceles trapezoidal $MgO:LiNbO_3$ crystal was used. The base angle of the trapezoidal crystal was 65° and its bottom length was 50 mm. The cavity and crystal length along the idler beam axis is half that of the cavity shown in Figure 1(a). To counteract the reduction in the gain length, the pump beam traverses the crystal twice. So, propagating length of the pump beam in the crystal is same as that of the cavity shown in Figure 1(a). M is a high-performance mirror that highly reflects (> 95%) only the idler wavelength and HR is a high-reflectivity dielectric mirror that highly reflects (> 98%) both the pump and idler beams. The pump laser was a Q-switched Nd:YAG laser with the pulse duration of 12 ns, maximum pulse energy of 500 mJ/pulse, and beam size of 8.0 mm.

THz pulse energy was measured by 4K Si-Bolometer. The generated THz-wave was focused on the 4-K Si bolometer through THz aspherical lens. The bolometer produces an output of 1 V for a (pulsed) input energy of 101 pJ with 200 times voltage amplify. The sensitivity for single shot was experimentally verified. When measuring the output, transmittance-calibrated thin metallized Mylar films were used to ensure that the output signal was below the saturation level of the bolometer.

3 RESULT AND DISCUSSIONS

Figure 2 shows the THz-wave output energy at 1.46 THz. The maximum output achieved was 382 nJ/pulse when the pump energy was 465 mJ/pulse and the pump beam was 8 mm in diameter. The inset of Figure 2 is magnified view for pump beams with sizes of 1.0 mm, 1.7 mm and 2.2 mm. The output from a SE-TPO has previously been reported to be 8 nJ/pulse for a pump energy of 23 mJ/pulse with a pump beam diameter of 1.0 mm [15]. The THz output energy was re-calibrated using latest sensitivity.

The approximately 50 times higher output energy achieved in the present study was obtained by increasing the pump energy by a factor of 20. The enhancement in the output energy exceeds linear scaling of the pump energy, indicating that the conversion efficiency was increased.

Figure 3(a) shows the dependence of the conversion efficiency on the pump fluence. A maximum conversion efficiency of 0.9×10^{-6} was achieved at a pump fluence of 0.92 J/cm^2 for a 8.0 mm pump beam, which corresponds to a pump energy of 465 mJ/pulse; these are the same conditions at which the maximum THz-wave output energy was observed. A conversion efficiency of 0.9×10^{-6} corresponds to a photon conversion ef-

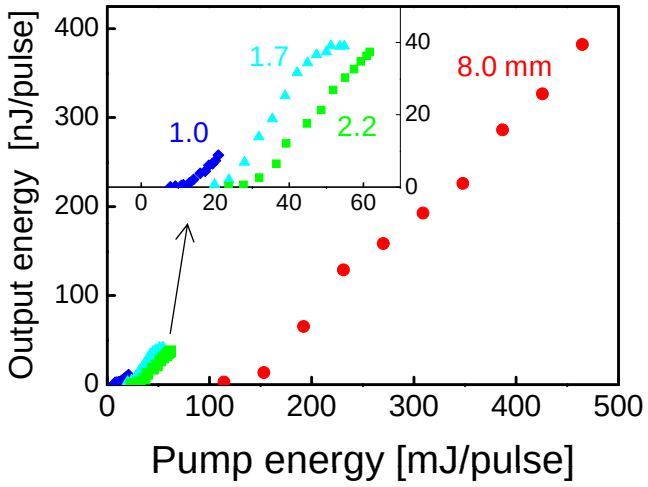

FIG. 2 THz output at various pump beam size and magnified view for pump beam size of 1.0 mm, 1.7 mm and 2.2 mm. The maximum output was obtained at 382 nJ/pulse, a pump beam size of 8.0 mm (FWHM) and 465 mJ/pulse.

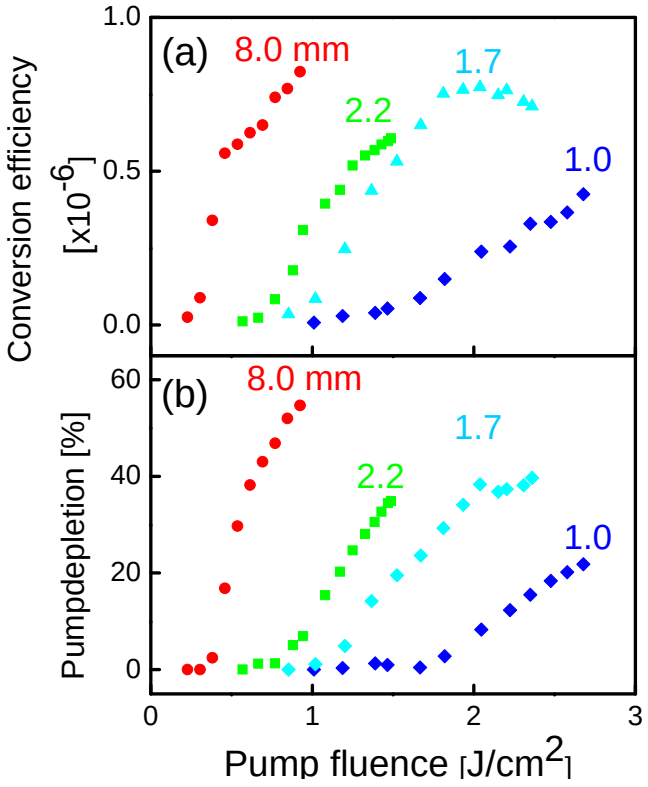

FIG. 3 (a) The THz-wave output conversion efficiency. (b) Pump depletion for various pump spot sizes. The figure shows a reduction in the threshold and an increase in the slope, indicating an improvement in the efficiency.

ficiency of 0.017%, since the frequency of the THz wave is 200 times lower than that of the pump beam. For the two smaller beam sizes, 1.0 mm and 1.7 mm, the maximum pump fluence was limited by the damage threshold of the crystal surfaces, which is typically about 2.6 J/cm^2. For the pump beam sizes of 2.0 mm and 8.0 mm, the maximum input energy was limited by the available Nd:YAG laser output pulse energy of 60 mJ and 500 mJ respectively.

Figure 3(b) shows the dependence of the pump depletion on the pump beam size when 1.46 THz was generated. We define

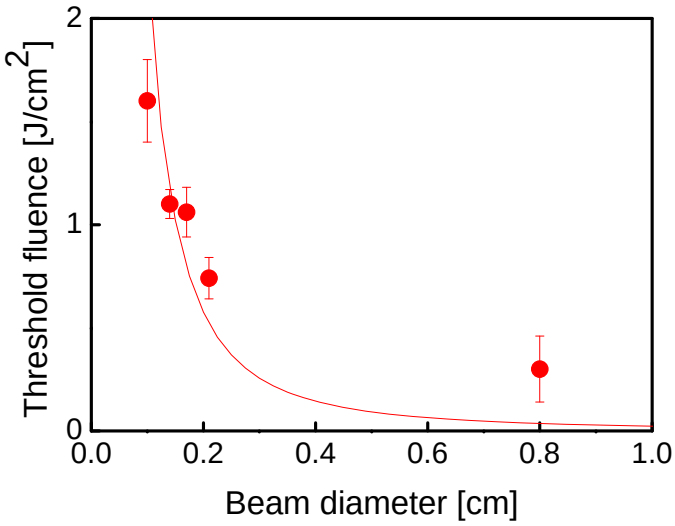

FIG. 4 Measured threshold fluence at difference beam spot sizes. The solid line is a fitted curve based on an inverse quadratic function.

the pump depletion as:

$$H \approx (E_m - E_a)/E_m \quad (1)$$

where E_m is the pump pulse energy after it has passed through the misaligned cavity and E_a is the pump energy after it has passed through the aligned cavity. When the cavity is aligned, the reduction of pump energy was observed. The some of pump energy was converted into idler and THz-wave energy. $E_a$is reduced energy due to the parametric conversion. In contrast, misaligning the cavity can suppress the nonlinear conversion. E_m is the input pump energy without depletion. The maximum observed pump depletion was 54% at a pump fluence of 0.92 J/cm^2 for a pump beam size of 8.0 mm. This is the largest depletion observed in our TPO research. Figures 3(a) and 3(b) show that the oscillation threshold decreases and the slope efficiency increases as the width of the pump beam is increased.

The spectral width was increased by increasing the pump beam size. The measured THz-wave spectral width estimated from the idler waves was greater than 500 GHz above 0.5 J/cm^2 when a pump beam size of 8.0 mm was used. Injection seeding or an intracavity grazing-incidence grating could be used to reduce the spectral width [12].

Figure 4 shows a reduction in the threshold. In a singly resonant OPO, the threshold is inversely proportional to the square of the effective interaction length [16]. The solid line is a fitted curve that is an inverse quadratic function of the beam size. The resonating idler and nonresonating THz beams are crossed with the pump beam using a noncollinear geometry. If we assume that the effective interaction length is proportional to the pump beam diameter and transverse interaction volume is not significant affect the threshold fluence, we can roughly estimate that the threshold is inversely proportional to the beam diameter. The threshold fluence reduces drastically in small beam diameter. This result shows that the improvement in the efficiency is due to increasing the interactions.

The merit of SE-TPO is energy scaling by expanding the radiation area with large aperture pumping. The investigation of the dependence of the output-coupling efficiency on the pump beam size is important to discuss the possibility of the further upscaling. The external efficiency (η) for a nonresonant wave as a function of pump depletion (H)is

$$\eta = \frac{\omega_{\mathrm{THz}}}{\omega_p} \cdot Loss^{-1} \cdot H \tag{2}$$

where *Loss* includes the absorption in the crystal and Fresnel reflection at the surface of the THz wave. From Eq. (2), we can estimate *Loss* by measuring the conversion efficiency η and the pump depletion H by considering $\omega_T/\omega_p = 5.2 \times 10^{-3}$. η and H can be obtained by simultaneous measurements and they are shown in Figures 3(a) and 3(b). The output-coupling efficiency (Tr) is given by the inverse of *Loss*. The output-coupling efficiency was measured for different beam diameters and it were ranges from $Tr = Loss^{-1} = 2.5 \times 10^{-4}$ to 5.0×10^{-4} for all beam diameters. This demonstrates that the transmission efficiency is not strongly dependent on the pump beam diameter, indicating that the energy can be scaled up further. We note that this results including the error related to the term of ω_T/ω_p in Eq. (2), because the relatively wide spectral bandwidth for 8.0 mm pump beam size, which was 500 GHz centered at 1.46 THz.

4 CONCLUSIONS

Unlike difference frequency generation, which requires a dual frequency tunable source, the TPO uses only a single laser. We proposed the method to utilize the full energy of a Nd:YAG laser to increase the output energy. We have shown that in the noncollinear phase matching geometry, the threshold fluence and pump depletion depend on the pump beam size. When the beam size is increased, the threshold fluence decreases and the pump depletion increases. With a large pump beam size (diameter: 8.0 mm) and a high pump energy, we obtained a pump depletion of 54% with 0.96 J/cm^2. We also demonstrated that the output coupling loss does not depended on the pump beam size in the SE configuration.

ACKNOWLEDGEMENTS

The authors thank Dr. C. Otani of RIKEN Sendai and Prof. K. Kawase of Nagoya University for discussions on bolometer calibration, and Prof. S. Okajima and Dr. K. Nakayama in Chubu University for providing the CW THz source for experimental verification of the bolometer sensitivity. The authors thank Mr. Shoji of Teraphotonics Laboratory at RIKEN Sendai for polishing the crystals and C. Takyu for coating the crystal surface.

References

[1] M. Tonouchi, "Cutting-edge terahertz technology" Nat. Photonics **1**, 97–105 (2007).

[2] H. Yoneyama, M. Yamashita, S. Kasai, K. Kawase, H. Ito, and T. Ouchi, "Membrane device for holding biomolecule samples for terahertz spectroscopy" Opt. Commun. **281**, 1909–1913 (2008).

[3] K. Kawase, Y. Ogawa, Y. Watanabe, and H. Inoue, "Non-destructive terahertz imaging of illicit drugs using spectral fingerprints" Opt. Express **11**, 2549–2554 (2003).

[4] K. Fukunaga, Y. Ogawa, S. Hayashi, and I. Hosako, "Terahertz spectroscopy for art conservation" IEICE Electron. Expr. **4**, 258–263 (2007).

[5] S. Ohno, A. Hamano, K. Miyamoto, K. Suzuki, and H. Ito, "Surface mapping of carrier density in a GaN wafer using a frequency-agile THz source" J. Europ. Opt. Soc. Rap. Public. **4**, 09012 (2009).

[6] M. A. Piestrup, R. N. Fleming, and R. H. Pantel, "Continuously tunable submillimeter wave source" Appl. Phys. Lett. **26**, 418–421 (1975).

[7] R. Guo, K. Akiyama, H. Minamide, and H. Ito, "Frequency-agile terahertz-wave spectrometer for high-resolution gas sensing" Appl. Phys. Lett. **90**, 121127 (2007).

[8] K. Kawase, J. Shikata, and H. Ito, "Terahertz wave parametric source" J. Phys. D Appl. Phys. **35**, R1–R14 (2002).

[9] K. Kawase, K. Nakamura, M. Sato, T. Taniuchi, and H. Ito, "Unidirectional radiation of widely tunable THz wave using a prism coupler under noncollinear phase matching condition" Appl. Phys. Lett. **71**, 753–755 (1997).

[10] Y. Watanabe, K. Kawase, T. Ikari, H. Ito, Y. Ishikawa, and H. Minamide, "Component spatial pattern analysis of chemicals using terahertz spectroscopic imaging" Appl. Phys. Lett. **83**, 800–802 (2003).

[11] J. Shikata, M. Sato, T. Taniuchi, H. Ito, and K. Kawase, "Enhancement of terahertz-wave output from $LiNbO_3$ optical parametric oscillators by cryogenic cooling" Opt. Lett. 24, 202–204 (1999).

[12] A. C. Chiang, T. D. Wang, Y. Y. Lin, S. T. Lin, H. H. Lee, Y. C. Huang, and Y. H. Chen, "Enhanced terahertz-wave parametric generation and oscillation in lithium niobate waveguides at terahertz frequencies" Opt. Lett. **30**, 3392–3394 (2005).

[13] S. Hayashi, H. Minamide, T. Ikari, Y. Ogawa, J. Shikata, H. Ito, C. Otani, and K. Kawase, "Output power enhancement of a palm-top terahertz-wave parametric generator" Appl. Opt. **46**, 117–123 (2007).

[14] S. J. Brosnan, and R. L. Byer, "Optical parametric oscillator threshold and linewidth studies" IEEE J. Quantum Elect. **15**, 415–431 (1976).

[15] T. Ikari, X. B. Zhang, H. Minamide, and H. Ito, "THz-wave parametric oscillator in surface emitted configuration" Opt. Express **14**, 1604–1610 (2006).

[16] R. G. Smith, "Optical parametric oscillators" in *Lasers: A Series of Advances*, A. K. Levine, A. J. DeMaria, eds., 189–307 (Dekker, New York, 1976).